nature

https://doi.org/10.1038/s41586-021-04388-0

Accelerated Article Preview

Striking Antibody Evasion Manifested by the Omicron Variant of SARS-CoV-2

Received: 14 December 2021

Accepted: 23 December 2021

Accelerated Article Preview Published online 23 December 2021

Cite this article as: Liu, L. et al. Striking Antibody Evasion Manifested by the Omicron Variant of SARS-CoV-2. *Nature* https://doi.org/10.1038/s41586-021-04388-0 (2021).

Lihong Liu, Sho Iketani, Yicheng Guo, Jasper F-W. Chan, Maple Wang, Liyuan Liu, Yang Luo, Hin Chu, Yiming Huang, Manoj S. Nair, Jian Yu, Kenn K-H. Chik, Terrence T-T. Yuen, Chaemin Yoon, Kelvin K-W. To, Honglin Chen, Michael T. Yin, Magdalena E. Sobieszczyk, Yaoxing Huang, Harris H. Wang, Zizhang Sheng, Kwok-Yung Yuen & David D. Ho

Article

Striking Antibody Evasion Manifested by the Omicron Variant of SARS-CoV-2

https://doi.org/10.1038/s41586-021-04388-0

Received: 14 December 2021

Accepted: 23 December 2021

Published online: 23 December 2021

Lihong Liu[1,7], Sho Iketani[1,2,7], Yicheng Guo[1,7], Jasper F-W. Chan[3,4,7], Maple Wang[1,7], Liyuan Liu[5,7], Yang Luo[1], Hin Chu[3,4], Yiming Huang[5], Manoj S. Nair[1], Jian Yu[1], Kenn K-H. Chik[4], Terrence T-T. Yuen[3], Chaemin Yoon[3], Kelvin K-W. To[3,4], Honglin Chen[3,4], Michael T. Yin[1,6], Magdalena E. Sobieszczyk[1,6], Yaoxing Huang[1], Harris H. Wang[5], Zizhang Sheng[1], Kwok-Yung Yuen[3,4] & David D. Ho[1,2,6]✉

The Omicron (B.1.1.529) variant of SARS-CoV-2 (severe acute respiratory syndrome coronavirus 2) was only recently detected in southern Africa, but its subsequent spread has been extensive, both regionally and globally[1]. It is expected to become dominant in the coming weeks[2], probably due to enhanced transmissibility. A striking feature of this variant is the large number of spike mutations[3] that pose a threat to the efficacy of current COVID-19 (coronavirus disease 2019) vaccines and antibody therapies[4]. This concern is amplified by the findings from our study. We found B.1.1.529 to be markedly resistant to neutralization by serum not only from convalescent patients, but also from individuals vaccinated with one of the four widely used COVID-19 vaccines. Even serum from persons vaccinated and boosted with mRNA-based vaccines exhibited substantially diminished neutralizing activity against B.1.1.529. By evaluating a panel of monoclonal antibodies to all known epitope clusters on the spike protein, we noted that the activity of 17 of the 19 antibodies tested were either abolished or impaired, including ones currently authorized or approved for use in patients. In addition, we also identified four new spike mutations (S371L, N440K, G446S, and Q493R) that confer greater antibody resistance to B.1.1.529. The Omicron variant presents a serious threat to many existing COVID-19 vaccines and therapies, compelling the development of new interventions that anticipate the evolutionary trajectory of SARS-CoV-2.

The COVID-19 (coronavirus disease 2019) pandemic rages on, as the causative agent, SARS-CoV-2 (severe acute respiratory syndrome coronavirus 2), continues to evolve. Many diverse viral variants have emerged (Fig. 1a), each characterized by mutations in the spike protein that raise concerns of both antibody evasion and enhanced transmission. The Beta (B.1.351) variant was found to be most refractory to antibody neutralization[4] and thus compromised the efficacy of vaccines[5–7] and therapeutic antibodies. The Alpha (B.1.1.7) variant became dominant globally in early 2021 due to an edge in transmission[8] only to be replaced by the Delta (B.1.617.2) variant, which exhibited even greater propensity to spread coupled with a moderate level of antibody resistance[9]. Then came the Omicron (B.1.1.529) variant, first detected in southern Africa in November 2021[3,10,11] (Fig. 1a). It has since spread rapidly in the region, as well as to over 60 countries, gaining traction even where the Delta variant is prevalent. The short doubling time (2-3 days) of Omicron cases suggests it could become dominant soon[2]. Moreover, its spike protein contains an alarming number of >30 mutations (Fig. 1b and Extended Data Fig. 1), including at least 15 in the receptor-binding domain (RBD), the principal target for neutralizing antibodies. These extensive spike mutations raise the specter that current vaccines and therapeutic antibodies would be greatly compromised. This concern is amplified by the findings we now report.

Serum neutralization of B.1.1.529

We first examined the neutralizing activity of serum collected in the Spring of 2020 from COVID-19 patients, who were presumably infected with the wild-type SARS-CoV-2 (9-120 days post-symptoms) (see Methods and Extended Data Table 1). Samples from 10 individuals were tested for neutralization against both D614G (WT) and B.1.1.529 pseudoviruses. While robust titers were observed against D614G, a significant drop (>32-fold) in ID_{50} (50% infectious dose) titers was observed against B.1.1.529, with only 2 samples showing titers above the limit of detection (LOD) (Fig. 1c and Extended Data Fig. 2a). We then assessed the neutralizing activity of sera from individuals who received one of the four widely used COVID-19 vaccines: BNT162b2 (Pfizer, 15-213 days

[1]Aaron Diamond AIDS Research Center, Columbia University Vagelos College of Physicians and Surgeons, New York, NY, 10032, USA. [2]Department of Microbiology and Immunology, Columbia University Vagelos College of Physicians and Surgeons, New York, NY, 10032, USA. [3]State Key Laboratory of Emerging Infectious Diseases, Carol Yu Centre for Infection, Department of Microbiology, Li Ka Shing Faculty of Medicine, The University of Hong Kong, Pokfulam, Hong Kong Special Administrative Region, Hong Kong, China. [4]Centre for Virology, Vaccinology and Therapeutics, Hong Kong Science and Technology Park, Hong Kong Special Administrative Region, Hong Kong, China. [5]Department of Systems Biology, Columbia University Vagelos College of Physicians and Surgeons, New York, NY, 10032, USA. [6]Division of Infectious Diseases, Department of Medicine, Columbia University Vagelos College of Physicians and Surgeons, New York, NY, 10032, USA. [7]These authors contributed equally: Lihong Liu, Sho Iketani, Yicheng Guo, Jasper F-W. Chan, Maple Wang, Liyuan Liu. ✉e-mail: dh2994@cumc.columbia.edu

post-vaccination), mRNA-1273 (Moderna, 6-177 days post-vaccination), Ad26.COV2.S (Johnson & Johnson, 50-186 days post-vaccination), and ChAdOx1 nCoV-19 (AstraZeneca, 91-159 days post-vaccination) (see Methods and Extended Data Table 2). In all cases, a substantial loss in neutralizing potency was observed against B.1.1.529 (Fig. 1d and Extended Data Fig. 2b-f). For the two mRNA-based vaccines, BNT162b2 and mRNA-1273, a >21-fold and >8.6-fold decrease in ID_{50} was seen, respectively. We note that, for these two groups, we specifically chose samples with high titers such that the fold-change in titer could be better quantified, so the difference in the number of samples having titers above the LOD (6/13 for BNT162b2 versus 11/12 for mRNA-1273) may be favorably biased. Within the Ad26.COV2.S and ChAdOx1 nCOV-19 groups, all samples were below the LOD against B.1.1.529, except for two Ad26.COV2.S samples from patients with a previous history of SARS-CoV-2 infection (Fig. 1d). Collectively, these results suggest that individuals who were previously infected or fully vaccinated remain at risk for B.1.1.529 infection.

Booster shots are now routinely administered in many countries 6 months after full vaccination. Therefore, we also examined the serum neutralizing activity of individuals who had received three homologous mRNA vaccinations (13 with BNT162b2 and 2 with mRNA-1273, 14-90 days post-vaccination). Every sample showed lower activity in neutralizing B.1.1.529, with a mean drop of 6.5-fold compared to WT (Fig. 1d). Although all samples had titers above the LOD, the substantial loss in activity may still pose a risk for B.1.1.529 infection despite the booster vaccination.

We then confirmed the above findings by testing a subset of the BNT162b2 and mRNA-1273 vaccinee serum samples using authentic SARS-CoV-2 isolates: wild type and B.1.1.529. Again, a substantial decrease in neutralization of B.1.1.529 was observed, with mean drops of >6.0-fold and >4.1-fold for the fully vaccinated group and the boosted group, respectively (Fig. 1e).

Antibody neutralization of B.1.1.529

To understand the types of antibodies in serum that lost neutralizing activity against B.1.1.529, we assessed the neutralization profile of 19 well-characterized monoclonal antibodies (mAbs) to the spike protein, including 17 directed to RBD and 2 directed to the N-terminal domain (NTD). We included mAbs that have been authorized or approved for clinical use, either individually or in combination: REGN10987 (imdevimab)[12], REGN10933 (casirivimab)[12], COV2-2196 (tixagevimab)[13], COV2-2130 (cilgavimab)[13], LY-CoV555 (bamlanivimab)[14], CB6 (etesevimab)[15], Brii-196 (amubarvimab)[16], Brii-198 (romlusevimab)[16], and S309 (sotrovimab)[17]. We also included other mAbs of interest: 910-30[18], ADG-2[19], DH1047[20], S2X259[21], and our antibodies 1-20, 2-15, 2-7, 4-18, 5-7, and 10-40[22–24]. The footprints of mAbs with structures available were drawn in relation to the mutations found in B.1.1.529 RBD (Fig. 2a) and NTD (Fig. 2b). The risk to each of the 4 classes[25] of RBD mAbs, as well as to the NTD mAbs, was immediately apparent. Indeed, neutralization studies on B.1.1.529 pseudovirus showed that 17 of the 19 mAbs tested lost neutralizing activity completely or partially (Fig. 2c and Extended Data Fig. 3). The potency of class 1 and class 2 RBD mAbs all dropped by >100-fold, as did the more potent mAbs in RBD class 3 (REGN10987, COV2-2130, and 2-7). The activities of S309 and Brii-198 were spared. All mAbs in RBD class 4 lost neutralization potency against B.1.1.529 by at least 10-fold, as did mAb directed to the antigenic supersite[26] (4-18) or the alternate site[23] (5-7) on NTD. Strikingly, all four combination mAb drugs in clinical use lost substantial activity against B.1.1.529, likely abolishing or impairing their efficacy in patients.

Approximately 10% of the B.1.1.529 viruses in GISAID[1] (Global Initiative on Sharing All Influenza Data) also contain an additional RBD mutation, R346K, which is the defining mutation for the Mu (B.1.621) variant[27]. We therefore constructed another pseudovirus (B.1.1.529+R346K) containing this mutation for additional testing using the same panel of mAbs (Fig. 2d). The overall findings resembled those already shown in Fig. 2c, with the exception that the neutralizing activity of Brii-198 was abolished. In fact, nearly the entire panel of antibodies was essentially rendered inactive against this minor form of the Omicron variant.

The fold changes in IC_{50} of the mAbs against B.1.1.529 and B.1.1.529+R346K relative to D614G are summarized in the first two rows of Fig. 3a. The remarkable loss of activity observed for all classes of mAbs against B.1.1.529 suggest that perhaps the same is occurring in the serum of convalescent patients and vaccinated individuals.

Mutations conferring antibody resistance

To understand the specific B.1.1.529 mutations that confer antibody resistance, we next tested individually the same panel of 19 mAbs against pseudoviruses for each of the 34 mutations (excluding D614G) found in B.1.1.529 or B.1.1.529+R346K. Our findings not only confirmed the role of known mutations at spike residues 142-145, 417, 484, and 501 in conferring resistance to NTD or RBD (class 1 or class 2) antibodies[4] but also revealed several mutations that were previously not known to have functional importance to neutralization (Fig. 3a and Extended Data Fig. 4). Q493R, previously shown to affect binding of CB6 and LY-CoV555[28] as well as polyclonal sera[29], mediated resistance to CB6 (class 1) as well as to LY-CoV555 and 2-15 (class 2), findings that could be explained by the abolishment of hydrogen bonds due to the long side chain of arginine and induced steric clashes with CDRH3 in these antibodies (Fig. 3b, **left panels**). Both N440K and G446S mediated resistance to REGN10987 and 2-7 (class 3), observations that could also be explained by steric hindrance (Fig. 3b, **middle panels**). The most striking and perhaps unexpected finding was that S371L broadly affected neutralization by mAbs in all 4 RBD classes (Fig. 3a and Extended Data Fig. 4). While the precise mechanism of this resistance is unknown, in silico modeling suggested two possibilities (Fig. 3b, **right panels**). First, in the RBD-down state, mutating Ser to Leu results in an interference with the N343 glycan, thereby possibly altering its conformation and affecting class 3 antibodies that typically bind this region. Second, in the RBD-up state, S371L may alter the local conformation of the loop consisting of S371-S373-S375, thereby affecting the binding of class 4 antibodies that generally target a portion of this loop[24]. It is not clear how class 1 and class 2 RBD mAbs are affected by this mutation.

Evolution of SARS-CoV-2 to antibodies

To gain insight into the antibody resistance of B.1.1.529 relative to previous SARS-CoV-2 variants, we evaluated the neutralizing activity of the same panel of neutralizing mAbs against pseudoviruses for B.1.1.7[8], B.1.526[30], B.1.429[31], B.1.617.2[9], P.1[32], and B.1.351[33]. It is evident from these results (Fig. 4 and Extended Data Fig. 5) that previous variants developed resistance only to NTD antibodies and class 1 and class 2 RBD antibodies. Here B.1.1.529, with or without R346K, has made a big mutational leap by becoming not only nearly completely resistant to class 1 and class 2 RBD antibodies, but also substantial resistance to both class 3 and class 4 RBD antibodies. B.1.1.529 is now the most complete "escapee" from neutralization by currently available antibodies.

Discussion

The Omicron variant struck fear almost as soon as it was detected to be spreading in South Africa. That this new variant would transmit more readily has come true in the ensuing weeks[2]. The extensive mutations found in its spike protein raised concerns that the efficacy of current COVID-19 vaccines and antibody therapies might be compromised. Indeed, in this study, sera from convalescent patients (Fig. 1c) and vaccinees (Figs. 1d and 1e) showed markedly reduced neutralizing activity against B.1.1.529. Other studies have found similar losses[34–38]. These findings are in line with emerging clinical data on the Omicron

variant demonstrating higher rates of reinfection[11] and vaccine breakthroughs. In fact, recent reports showed that the efficacy of two doses of BNT162b2 vaccine has dropped from over 90% against the original SARS-CoV-2 strain to approximately 40% and 33% against B.1.1.529 in the United Kingdom[39] and South Africa[40], respectively. Even a third booster shot may not adequately protect against Omicron infection[39,41], although the protection against disease still makes it advisable to administer booster vaccinations. Vaccines that elicited lower neutralizing titers[35,42] are expected to fare worse against B.1.1.529.

The nature of the loss in serum neutralizing activity against B.1.1.529 could be discerned from our findings on a panel of mAbs directed to the viral spike. The neutralizing activities of all four major classes of RBD mAbs and two distinct classes of NTD mAbs are either abolished or impaired (Figs. 2c and 2d). In addition to previously identified mutations that confer antibody resistance[4], we have uncovered four new spike mutations with functional consequences. Q493R confers resistance to some class 1 and class 2 RBD mAbs; N440K and G446S confer resistance to some class 3 RBD mAbs; and S371L confers global resistance to many RBD mAbs via mechanisms that are not yet apparent. While performing these mAb studies, we also observed that nearly all the currently authorized or approved mAb drugs are rendered weak or inactive by B.1.1.529 (Figs. 2c and 3a). In fact, the Omicron variant that contains R346K almost flattens the antibody therapy landscape for COVID-19 (Fig. 2d and 3a).

The scientific community has chased after SARS-CoV-2 variants for a year. As more and more of them appeared, our interventions directed to the spike became increasingly ineffective. The Omicron variant has now put an exclamation mark on this point. It is not too far-fetched to think that this SARS-CoV-2 is now only a mutation or two away from being pan-resistant to current antibodies, either monoclonal or polyclonal. We must devise strategies that anticipate the evolutional direction of the virus and develop agents that target better conserved viral elements.

Online content

Any methods, additional references, Nature Research reporting summaries, source data, extended data, supplementary information, acknowledgements, peer review information; details of author contributions and competing interests; and statements of data and code availability are available at https://doi.org/10.1038/s41586-021-04388-0.

1. Shu, Y. & McCauley, J. GISAID: Global initiative on sharing all influenza data - from vision to reality. *Euro Surveill* **22**, https://doi.org/10.2807/1560-7917.ES.2017.22.13.30494 (2017).
2. Grabowski, F., Kochańczyk, M. & Lipniacki, T. Omicron strain spreads with the doubling time of 3.2—3.6 days in South Africa province of Gauteng that achieved herd immunity to Delta variant. *medRxiv*, https://doi.org/10.1101/2021.12.08.21267494 (2021).
3. Scott, L. et al. Track Omicron's spread with molecular data. *Science*, eabn4543, https://doi.org/10.1126/science.abn4543 (2021).
4. Wang, P. et al. Antibody resistance of SARS-CoV-2 variants B.1.351 and B.1.1.7. *Nature* **593**, 130-135, https://doi.org/10.1038/s41586-021-03398-2 (2021).
5. Abu-Raddad, L. J., Chemaitelly, H., Butt, A. A. &National Study Group for, C.-V. Effectiveness of the BNT162b2 Covid-19 Vaccine against the B.1.1.7 and B.1.351 Variants. *N Engl J Med* **385**, 187-189, https://doi.org/10.1056/NEJMc2104974 (2021).
6. Madhi, S. A. et al. Efficacy of the ChAdOx1 nCoV-19 Covid-19 Vaccine against the B.1.351 Variant. *N Engl J Med* **384**, 1885-1898, https://doi.org/10.1056/NEJMoa2102214 (2021).
7. Sadoff, J. et al. Safety and Efficacy of Single-Dose Ad26.COV2.S Vaccine against Covid-19. *N Engl J Med* **384**, 2187-2201, https://doi.org/10.1056/NEJMoa2101544 (2021).
8. Davies, N. G. et al. Estimated transmissibility and impact of SARS-CoV-2 lineage B.1.1.7 in England. *Science* **372**, https://doi.org/10.1126/science.abg3055 (2021).
9. Mlcochova, P. et al. SARS-CoV-2 B.1.617.2 Delta variant replication and immune evasion. *Nature* **599**, 114-119, https://doi.org/10.1038/s41586-021-03944-y (2021).
10. Hadfield, J. et al. Nextstrain: real-time tracking of pathogen evolution. *Bioinformatics* **34**, 4121-4123, https://doi.org/10.1093/bioinformatics/bty407 (2018).
11. Pulliam, J. R. C. et al. Increased risk of SARS-CoV-2 reinfection associated with emergence of the Omicron variant in South Africa. *medRxiv*, https://doi.org/10.1101/2021.11.11.21266068 (2021).
12. Hansen, J. et al. Studies in humanized mice and convalescent humans yield a SARS-CoV-2 antibody cocktail. *Science* **369**, 1010-1014, https://doi.org/10.1126/science.abd0827 (2020).
13. Zost, S. J. et al. Potently neutralizing and protective human antibodies against SARS-CoV-2. *Nature* **584**, 443-449, https://doi.org/10.1038/s41586-020-2548-6 (2020).
14. Jones, B. E. et al. The neutralizing antibody, LY-CoV555, protects against SARS-CoV-2 infection in nonhuman primates. *Sci Transl Med* **13**, https://doi.org/10.1126/scitranslmed.abf1906 (2021).
15. Shi, R. et al. A human neutralizing antibody targets the receptor-binding site of SARS-CoV-2. *Nature* **584**, 120-124, https://doi.org/10.1038/s41586-020-2381-y (2020).
16. Ju, B. et al. Human neutralizing antibodies elicited by SARS-CoV-2 infection. *Nature* **584**, 115-119, https://doi.org/10.1038/s41586-020-2380-z (2020).
17. Pinto, D. et al. Cross-neutralization of SARS-CoV-2 by a human monoclonal SARS-CoV antibody. *Nature* **583**, 290-295, https://doi.org/10.1038/s41586-020-2349-y (2020).
18. Banach, B. B. et al. Paired heavy- and light-chain signatures contribute to potent SARS-CoV-2 neutralization in public antibody responses. *Cell Rep* **37**, 109771, https://doi.org/10.1016/j.celrep.2021.109771 (2021).
19. Rappazzo, C. G. et al. Broad and potent activity against SARS-like viruses by an engineered human monoclonal antibody. *Science* **371**, 823-829, https://doi.org/10.1126/science.abf4830 (2021).
20. Li, D. et al. In vitro and in vivo functions of SARS-CoV-2 infection-enhancing and neutralizing antibodies. *Cell* **184**, 4203-4219 e4232, https://doi.org/10.1016/j.cell.2021.06.021 (2021).
21. Tortorici, M. A. et al. Broad sarbecovirus neutralization by a human monoclonal antibody. *Nature* **597**, 103-108, https://doi.org/10.1038/s41586-021-03817-4 (2021).
22. Liu, L. et al. Potent neutralizing antibodies against multiple epitopes on SARS-CoV-2 spike. *Nature* **584**, 450-456, https://doi.org/10.1038/s41586-020-2571-7 (2020).
23. Cerutti, G. et al. Neutralizing antibody 5-7 defines a distinct site of vulnerability in SARS-CoV-2 spike N-terminal domain. *Cell Rep* **37**, 109928, https://doi.org/10.1016/j.celrep.2021.109928 (2021).
24. Liu, L. et al. Isolation and comparative analysis of antibodies that broadly neutralize sarbecoviruses. *bioRxiv*, https://doi.org/10.1101/2021.12.11.472236 (2021).
25. Barnes, C. O. et al. SARS-CoV-2 neutralizing antibody structures inform therapeutic strategies. *Nature* **588**, 682-687, https://doi.org/10.1038/s41586-020-2852-1 (2020).
26. Cerutti, G. et al. Potent SARS-CoV-2 neutralizing antibodies directed against spike N-terminal domain target a single supersite. *Cell Host Microbe* **29**, 819-833 e817, https://doi.org/10.1016/j.chom.2021.03.005 (2021).
27. Uriu, K. et al. Neutralization of the SARS-CoV-2 Mu Variant by Convalescent and Vaccine Serum. *N Engl J Med*, https://doi.org/10.1056/NEJMc2114706 (2021).
28. Starr, T. N., Greaney, A. J., Dingens, A. S. & Bloom, J. D. Complete map of SARS-CoV-2 RBD mutations that escape the monoclonal antibody LY-CoV555 and its cocktail with LY-CoV016. *Cell Rep Med* **2**, 100255, https://doi.org/10.1016/j.xcrm.2021.100255 (2021).
29. Amanat, F. et al. SARS-CoV-2 mRNA vaccination induces functionally diverse antibodies to NTD, RBD, and S2. *Cell* **184**, 3936-3948 e3910, https://doi.org/10.1016/j.cell.2021.06.005 (2021).
30. Annavajhala, M. K. et al. Emergence and expansion of SARS-CoV-2 B.1.526 after identification in New York. *Nature* **597**, 703-708, https://doi.org/10.1038/s41586-021-03908-2 (2021).
31. Zhang, W. et al. Emergence of a Novel SARS-CoV-2 Variant in Southern California. *JAMA* **325**, 1324-1326, https://doi.org/10.1001/jama.2021.1612 (2021).
32. Faria, N. R. et al. Genomics and epidemiology of the P.1 SARS-CoV-2 lineage in Manaus, Brazil. *Science* **372**, 815-821, https://doi.org/10.1126/science.abh2644 (2021).
33. Tegally, H. et al. Detection of a SARS-CoV-2 variant of concern in South Africa. *Nature* **592**, 438-443, https://doi.org/10.1038/s41586-021-03402-9 (2021).
34. Schmidt, F. et al. Plasma neutralization properties of the SARS-CoV-2 Omicron variant. *medRxiv* (2021).
35. Garcia-Beltran, W. F. et al. mRNA-based COVID-19 vaccine boosters induce neutralizing immunity against SARS-CoV-2 Omicron variant. *medRxiv*, https://doi.org/10.1101/2021.12.14.21267755 (2021).
36. Cameroni, E. et al. Broadly neutralizing antibodies overcome SARS-CoV-2 Omicron antigenic shift. *bioRxiv* (2021).
37. Doria-Rose, N. A. et al. Booster of mRNA-1273 Vaccine Reduces SARS-CoV-2 Omicron Escape from Neutralizing Antibodies. *medRxiv* (2021).
38. Planas, D. et al. Considerable escape of SARS-CoV-2 variant Omicron to antibody neutralization. *bioRxiv* (2021).
39. Andrews, N. et al. Effectiveness of COVID-19 vaccines against the Omicron (B.1.1.529) variant of concern. *medRxiv*, https://doi.org/10.1101/2021.12.14.21267615 (2021).
40. Wroughton, L. in *The Washington Post* (2021).
41. Kuhlmann, C. et al. Breakthrough Infections with SARS-CoV-2 Omicron Variant Despite Booster Dose of mRNA Vaccine. *SSRN*, https://doi.org/10.2139/ssrn.3981711 (2021).
42. Cromer, D. et al. Neutralising antibody titres as predictors of protection against SARS-CoV-2 variants and the impact of boosting: a meta-analysis. *Lancet Microbe*, https://doi.org/10.1016/S2666-5247(21)00267-6 (2021).

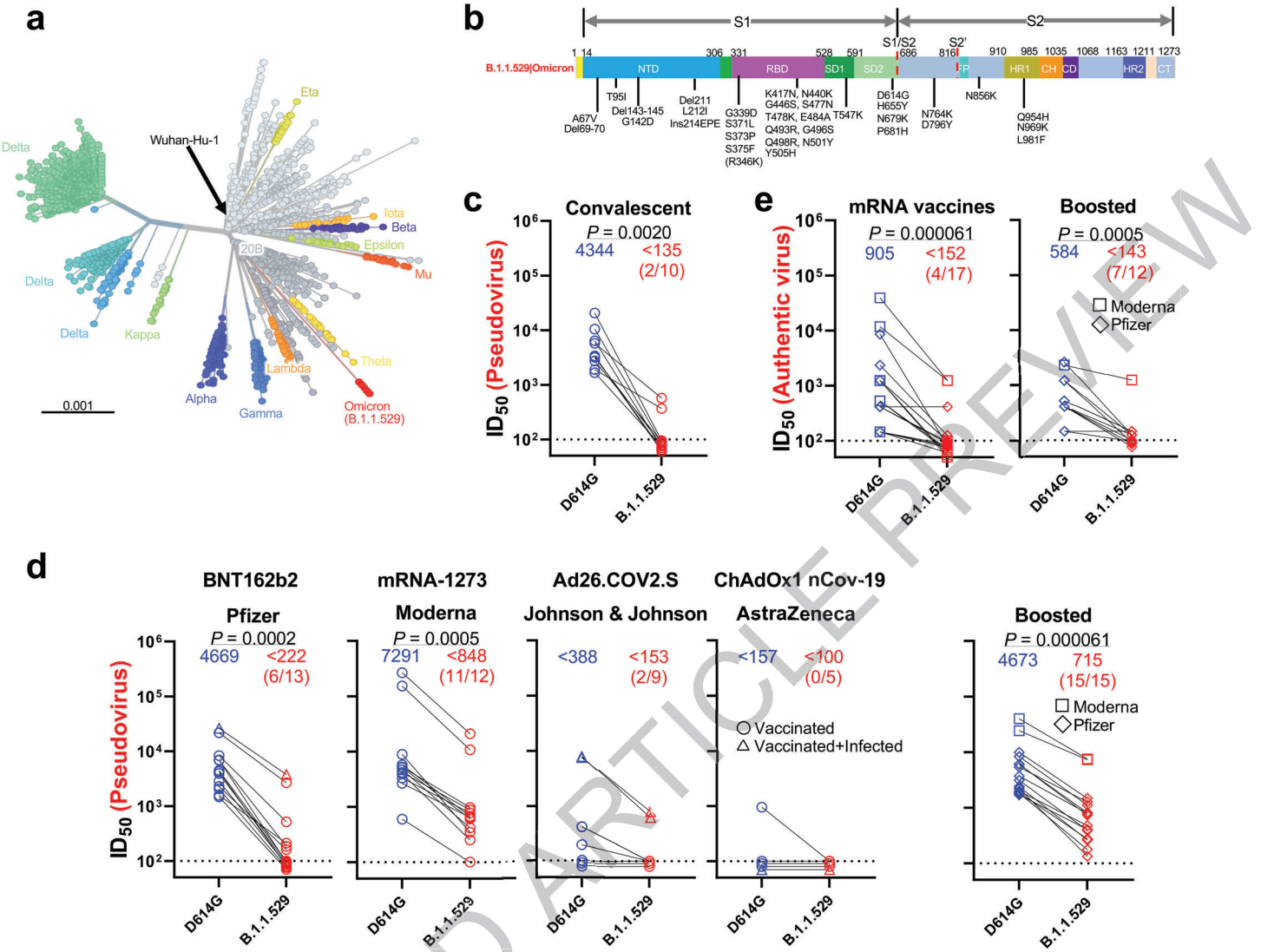

Fig. 1 | Resistance of B.1.1.529 to neutralization by sera. a, Unrooted phylogenetic tree of B.1.1.529 with other major SARS-CoV-2 variants. **b**, Key spike mutations found in the viruses isolated in the major lineage of B.1.1.529 are denoted. **c**, Neutralization of D614G and B.1.1.529 pseudoviruses by convalescent patient sera. **d**, Neutralization of D614G and B.1.1.529 pseudoviruses by vaccinee sera. Within the four standard vaccination groups, individuals that were vaccinated without documented infection are denoted as circles and individuals that were both vaccinated and infected are denoted as triangles. Within the boosted group, Moderna vaccinees are denoted as squares and Pfizer vaccinees are denoted as diamonds. **e**, Neutralization of authentic D614G and B.1.1.529 viruses by vaccinee sera. Moderna vaccinees are denoted as squares and Pfizer vaccinees are denoted as diamonds. Data represent one of two independent experiments. For all panels, values above the symbols denote geometric mean titer and the numbers in parentheses denote the number of samples above the limit of detection. *P* values were determined by using a Wilcoxon matched-pairs signed-rank test (two-tailed).

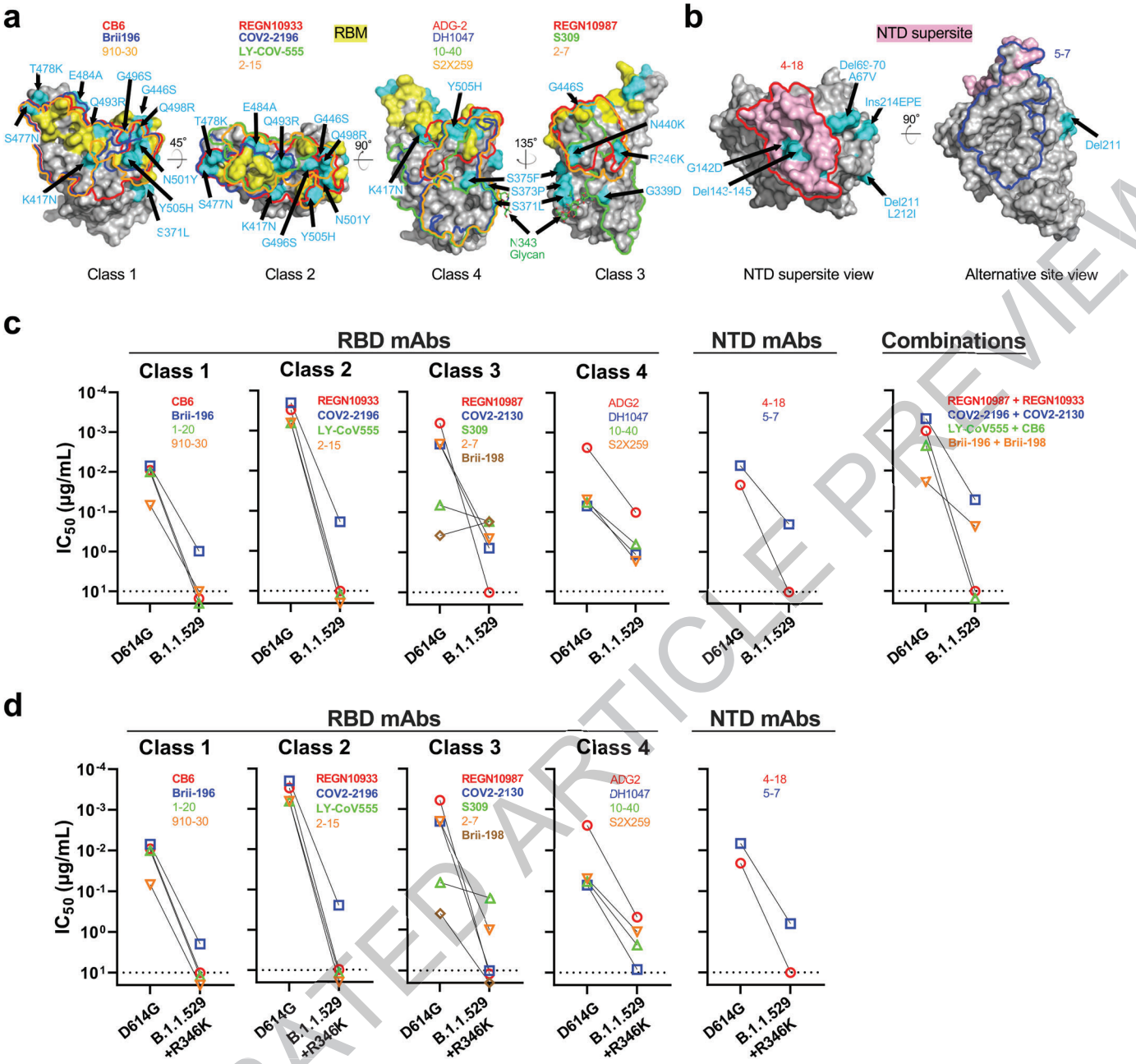

Fig. 2 | Resistance of B.1.1.529 to neutralization by monoclonal antibodies. **a**, Footprints of RBD-directed antibodies, with mutations within B.1.1.529 highlighted in cyan. Approved or authorized antibodies are bolded. The receptor binding motif (RBM) residues are highlighted in yellow. **b**, Footprints of NTD-directed antibodies, with mutations within B.1.1.529 highlighted in cyan. The NTD supersite residues are highlighted in light pink. **c**, Neutralization of D614G and B.1.1.529 pseudoviruses by RBD-directed and NTD-directed mAbs. **d**, Neutralization D614G and B.1.1.529+R346K pseudoviruses by RBD-directed and NTD-directed mAbs. Data represent one of two independent experiments.

a

Fold change in IC50 compared with WT	RBD mAbs																	NTD mAbs	
	Class 1				Class 2				Class 3					Class 4					
	CB6	Brii-196	1-20	910-30	REGN10933	COV2-2196	LY-CoV555	2-15	REGN10987	COV2-2130	S309	2-7	Brii-198	ADG-2	DH1047	10-40	S2X259	4-18	5-7
B.1.1.529	<-1000	-134	<-338	<-159	<-1000	-140	<-1000	<-1000	<-1000	-390	-2.5	-231	2.2	-43	-124	-11	-35	-125	-30
B.1.1.529 + R346K	<-761	-97	<-338	<-159	<-1000	-89	<-1000	<-1000	<-1000	<-988	-2.4	-109	<-32	-51	-167	-32	-16	-125	-33
A67V	1.1	1.0	-1.1	1.4	1.1	-1.0	1.1	1.1	1.1	1.2	-1.4	-1.1	-1.2	1.3	-1.3	-1.1	1.0	-1.6	-1.1
Del69-70	-1.4	-1.4	-1.6	-1.1	-1.8	-1.5	-1.4	-1.4	-1.7	-1.4	-2.2	-1.9	-2.3	-1.4	-3.3	-1.7	-1.3	-2.6	-9.4
T95I	-1.4	-2.0	-1.8	-1.7	-1.5	-1.6	-1.5	1.1	-2.0	-1.1	-2.3	-3.4	1.3	-2.5	-3.4	-1.9	-2.2	1.0	-9.5
G142D	-1.3	-1.4	-1.6	1.0	-1.6	-1.6	-1.7	-1.6	-1.9	-1.5	-2.9	-2.9	-1.5	-1.4	-2.8	-1.4	-1.5	<-125	-263
Del143-145	1.3	1.0	-1.2	1.4	1.3	1.6	1.3	1.5	1.1	-1.1	-1.9	1.2	-1.3	1.2	-2.0	-1.2	-1.2	<-125	-29
Del211	-2.4	-2.1	-1.6	-2.1	-1.5	-1.5	-1.4	-1.2	1.2	-1.2	-1.2	-1.3	-1.1	-1.9	-2.4	-1.6	-2.3	1.2	-9.1
L212I	-1.3	-1.8	-1.3	-1.6	-1.4	-1.4	-1.6	-1.3	-1.3	-1.4	-2.2	-1.9	-2.2	-1.7	-3.2	-2.0	-1.9	-7.2	-2.2
Ins214EPE	-2.4	-2.4	-2.2	-2.4	-2.8	-2.7	-2.3	-4.3	-3.0	-2.2	-3.0	-6.2	-2.7	-3.1	-2.9	-1.9	-3.3	-7.1	-15
G339D	-1.7	-1.6	-1.7	-1.4	-2.2	-1.7	-1.5	-1.4	-1.8	-1.6	-4.0	-1.9	-3.9	-1.6	-2.2	-1.5	-3.2	-4.5	-3.0
(R346K)	-1.5	-1.2	-1.3	1.0	-1.5	-1.3	-1.3	-1.4	-1.6	-2.9	-1.4	-1.0	-21	-1.1	-1.9	-1.2	-1.4	-1.4	-2.3
S371L	-19	-18	-15	-22	-10	-4.1	-2.9	-1.4	-25	-1.4	-12	-12	-17	-18	-49	-59	-23	-1.8	1.1
S373P	-1.9	-2.1	-1.6	-1.4	-1.9	-2.1	-2.0	-1.4	-1.9	-1.3	-2.3	-1.8	-2.5	-2.2	-5.1	-5.0	-2.8	-8.2	-5.0
S375F	1.7	1.6	1.6	1.5	2.1	1.9	1.9	2.6	1.2	1.5	-1.1	1.4	1.1	1.8	-1.8	-1.2	-1.6	-9.2	-1.6
K417N	<-761	-1.6	-2.3	<-158	-6.4	1.1	1.5	1.1	1.2	1.2	-1.8	1.5	-1.0	-1.1	-1.9	-1.5	-1.8	-5.3	-2.8
N440K	-1.4	-1.4	-1.6	-1.2	-1.7	-1.4	-1.4	-1.6	-246	-1.5	-2.3	-18	-1.6	1.1	-2.0	-1.3	-1.5	-4.3	-2.8
G446S	1.3	1.1	-1.1	1.2	-1.6	-1.1	-1.6	-3.0	-574	-3.7	-1.7	-50	-1.4	-1.6	-2.2	-1.4	-2.2	-3.9	-2.4
S477N	-1.8	-1.8	-1.7	-1.7	-2.4	-1.5	-1.5	-1.7	-2.9	-1.6	-1.9	-4.4	-2.4	-1.5	-2.3	-1.6	-2.2	-17	-5.1
T478K	1.2	1.1	1.4	1.6	1.3	-1.5	-1.4	-1.2	-1.6	1.1	-1.8	-2.6	-1.6	-1.2	-2.8	-1.3	-2.3	-3.3	-2.3
E484A	-2.8	-1.7	-1.8	-1.2	-4.8	-4.9	<-1000	<-1000	-1.6	-1.4	-1.4	-2.7	-1.9	-1.6	-1.5	-1.9	-1.9	-5.7	-2.9
Q493R	-16	-7.3	-3.2	2.9	-42	-4.2	<-1000	-705	-1.4	-1.1	-1.2	-1.9	-2.0	-1.6	-1.6	-1.6	-1.5	-4.0	-1.3
G496S	-1.3	1.3	1.1	1.1	1.0	1.1	1.0	-9.3	-6.2	-1.3	-1.4	1.4	-1.2	-1.2	-1.6	-1.1	-1.6	-2.6	-1.6
Q498R	-1.7	-1.2	1.1	1.4	-1.5	-1.1	-1.4	-1.0	-1.6	-1.4	-1.3	1.1	-1.2	2.4	-1.3	-1.2	-1.3	-1.5	-1.8
N501Y	-9.8	-1.2	-8.4	-16	-1.4	-1.5	-1.6	-1.2	-1.2	-1.1	-1.8	-1.5	-2.7	-1.8	-2.5	-1.9	-1.9	-20	-3.9
Y505H	-1.2	1.2	-1.3	-9.6	1.1	1.0	1.0	1.1	1.4	1.0	-1.4	1.7	1.1	1.3	-1.4	1.0	-1.2	-1.2	-1.1
T547K	-1.9	-2.0	-2.0	-1.9	-1.7	-1.3	-1.6	-1.7	-2.7	-1.6	-1.6	-4.3	-1.9	-1.7	-2.6	-1.5	-1.9	-2.7	-2.7
H655Y	-2.7	-3.1	-3.5	-2.7	-3.1	-2.0	-2.2	-8.6	-8.8	-1.7	-2.3	-13	-2.4	-2.1	-3.9	-3.3	-3.9	-23	-5.3
N679K	1.0	1.2	1.1	1.1	-1.1	-1.2	-1.2	-1.2	-1.9	-1.1	-1.3	-1.8	-1.7	-1.4	-2.4	-1.7	-1.7	-2.1	-2.7
P681H	-2.3	-2.1	-2.1	1.0	-2.4	-1.8	-2.2	-1.5	-1.5	-1.0	-1.6	-1.9	-1.5	-1.3	-2.3	-1.3	-1.3	-2.3	-2.4
N764K	-1.1	-1.5	-1.3	-1.1	-1.4	-1.4	-1.4	-2.1	-2.5	-1.5	-2.2	-4.3	-1.3	-1.4	-3.3	-2.1	-2.4	-2.3	-2.1
D769Y	1.3	1.1	1.0	1.2	-1.5	-1.0	-1.4	-1.4	-2.0	-1.3	-1.9	-2.5	-1.3	-1.1	-1.7	-1.2	-1.4	-3.1	-2.5
N856K	-10	-2.8	-1.3	-12	-2.2	-3.0	-1.1	-1.0	-1.4	-1.1	-1.2	-1.3	-2.3	-1.8	-4.4	-2.1	-2.5	-1.6	-1.9
Q954H	2.7	1.9	1.5	2.6	1.2	1.0	1.2	1.1	-1.1	1.2	-1.2	-1.4	-1.1	-1.1	-2.5	-1.0	-1.1	-2.3	-2.9
N969K	-5.4	-1.6	-1.1	-4.5	-1.3	-1.8	-1.1	-1.3	-1.6	-1.1	-1.4	-2.4	-1.4	-1.1	-2.3	-2.0	-2.4	-2.5	-2.0
L981F	3.2	3.3	2.1	4.6	2.4	2.5	2.2	1.9	1.3	2.5	-1.0	-1.5	8.6	2.8	1.1	2.0	2.1	-1.3	-1.5

Legend: >3 | <-3 | <-10 | <-100

b

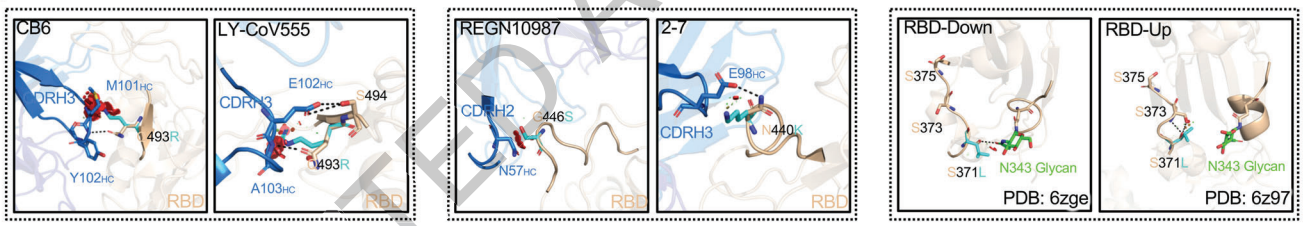

Fig. 3 | Impact of individual mutations within B.1.1.529 against monoclonal antibodies. a, Neutralization of pseudoviruses harboring single mutations found within B.1.1.529 by a panel of 19 monoclonal antibodies. Fold change relative to neutralization of D614G is denoted, with resistance colored red and sensitization colored green. **b**, Modeling of critical mutations in B.1.1.529 that affect antibody neutralization.

Fold change in IC50 compared with WT	RBD mAbs																	NTD mAbs	
	Class 1				Class 2				Class 3					Class 4					
	CB6	Brii-196	1-20	910-30	REGN10933	COV2-2196	LY-CoV555	2-15	REGN10987	COV2-2130	S309	2-7	Brii-198	ADG-2	DH1047	10-40	S2X259	4-18	5-7
B.1.1.7	-8.8	2.6	-5.2	-15	1.6	1.8	1.6	2.2	2.9	1.7	1.1	2.3	4.1	1.7	2.2	1.4	1.4	-5.1	-4.0
B.1.526	-1.0	1.1	-1.1	2.5	-4.5	-2.1	-590	-1329	1.8	1.2	2.9	1.8	-1.1	1.5	2.9	-2.2	1.4	4.5	-2.5
B.1.429	3.0	2.3	1.4	2.5	2.5	2.8	-590	-4.6	1.6	1.1	1.9	1.6	-2.4	2.0	2.9	1.3	3.3	-39	-59
B.1.617.2	2.1	1.2	-1.1	2.5	1.2	1.4	-590	-10	-1.8	-1.7	1.2	-1.1	-8.9	1.0	1.4	-1.8	-1.4	-39	-74
P.1	-196	2.2	-16	-60	-121	-2.0	-590	-1329	1.9	1.1	1.1	1.2	1.8	-1.0	3.0	-2.2	1.2	-39	-74
B.1.351	-196	2.0	-40	-60	-78	-2.5	-590	-1329	1.5	1.5	1.2	1.9	-1.5	1.0	3.0	-2.9	1.2	-39	-8.4
B.1.1.529	<-1000	-134	<-338	<-159	<-1000	-140	<-1000	<-1000	<-1000	-390	-2.5	-231	2.2	-43	-124	-11	-35	-125	-30
B.1.1.529 + R346K	<-761	-97	<-338	<-159	<-1000	-89	<-1000	<-1000	<-1000	<-988	-2.4	-109	<-32	-51	-167	-32	-16	-125	-33

Legend: >3 | <-3 | <-10 | <-100

Fig. 4 | Evolution of antibody resistance across SARS-CoV-2 variants. Neutralization of SARS-CoV-2 variant pseudoviruses by a panel of 19 monoclonal antibodies. Fold change relative to neutralization of D614G is denoted.

Methods

Data reporting

No statistical methods were used to predetermine sample size. The experiments were not randomized and the investigators were not blinded to allocation during experiments and outcome assessment.

Serum samples

Convalescent plasma samples were obtained from patients with documented SARS-CoV-2 infection. These samples were collected at the beginning of the pandemic in early 2020 at Columbia University Irving Medical Center, and therefore are assumed to be infection by the wild-type strain of SARS-CoV-2[4]. Sera from individuals who received two or three doses of mRNA-1273 or BNT162b2 vaccine were collected at Columbia University Irving Medical Center at least two weeks after the final dose. Sera from individuals who received one dose of Ad26.COV2.S or two doses of ChAdOx1 nCov-19 were obtained from BEI Resources. Some individuals were also infected by SARS-CoV-2 in addition to the vaccinations they received. Note that, whenever possible, we specifically chose samples with high titers against the wild-type strain of SARS-CoV-2 such that the loss in activity against B.1.1.529 could be better quantified, and therefore the titers observed here should be considered in that context. All collections were conducted under protocols reviewed and approved by the Institutional Review Board of Columbia University. All participants provided written informed consent. Additional information for the convalescent samples can be found in Extended Data Table 1 and for vaccinee samples can be found in Extended Data Table 2.

Monoclonal antibodies

Antibodies were expressed as previously described[22], by synthesis of heavy chain variable (VH) and light chain variable (VL) genes (GenScript), transfection of Expi293 cells (Thermo Fisher), and affinity purification from the supernatant by rProtein A Sepharose (GE). REGN10987, REGN10933, COV2-2196, and COV2-2130 were provided by Regeneron Pharmaceuticals, Brii-196 and Brii-198 were provided by Brii Biosciences, CB6 was provided by Baoshan Zhang and Peter Kwong (NIH), and 910-30 was provided by Brandon DeKosky (MIT).

Cell lines

Expi293 cells were obtained from Thermo Fisher (Catalog #A14527), Vero E6 cells were obtained from ATCC (Catalog# CRL-1586), HEK293T cells were obtained from ATCC (Catalog# CRL-3216), and Vero-E6-TMPRSS2 cells were obtained from JCRB (Catalog# JCRB1819). Cells were purchased from authenticated vendors and morphology was confirmed visually prior to use. All cell lines tested mycoplasma negative.

Variant SARS-CoV-2 spike plasmid construction

An in-house high-throughput template-guide gene synthesis approach was used to generate spike genes with single or full mutations of B.1.1.529. Briefly, 5′-phosphorylated oligos with designed mutations were annealed to the reverse strand of the wild-type spike gene construct and extended by DNA polymerase. Extension products (forward-stranded fragments) were then ligated together by Taq DNA ligase and subsequently amplified by PCR to generate variants of interest. To verify the sequences of variants, next generation sequencing (NGS) libraries were prepared following a low-volume Nextera sequencing protocol[43] and sequenced on the Illumina Miseq platform (single-end mode with 50 bp R1). Raw reads were processed by Cutadapt v2.1[44] with default setting to remove adapters and then aligned to reference variants sequences using Bowtie2 v2.3.4[45] with default setting. Resulting reads alignments were then visualized in Integrative Genomics Viewer[46] and subjected to manual inspection to verify the fidelity of variants. Sequences of the oligos used in variants generation are provided in Extended Data Table 3.

Pseudovirus production

Pseudoviruses were produced in the vesicular stomatitis virus (VSV) background, in which the native glycoprotein was replaced by that of SARS-CoV-2 and its variants, as previously described[24]. Briefly, HEK293T cells were transfected with a spike expression construct with polyethylenimine (PEI) (1 mg/mL) and cultured overnight at 37 °C under 5% CO_2, and then infected with VSV-G pseudotyped ΔG-luciferase (G*ΔG-luciferase, Kerafast) one day post-transfection. Following 2 h of infection, cells were washed three times, changed to fresh medium, and then cultured for approximately another 24 h before supernatants were collected, centrifuged, and aliquoted to use in assays.

Pseudovirus neutralization assay

All viruses were first titrated to normalize the viral input between assays. Heat-inactivated sera or antibodies were first serially diluted in 96 well-plates in triplicate, starting at 1:100 dilution for sera and 10 μg/mL for antibodies. Viruses were then added and the virus-sample mixture was incubated at 37 °C for 1 h. Vero-E6 cells (ATCC) were then added at a density of 3×10^4 cells per well and plates were incubated at 37 °C for approximately 10 h. Luciferase activity was quantified by using the Luciferase Assay System (Promega) according to the manufacturer's instructions using the software SoftMax Pro 7.0.2 (Molecular Devices, LLC). Neutralization curves and IC_{50} (50% inhibitory concentration) values were derived by fitting a non-linear five-parameter dose-response curve to the data in GraphPad Prism version 9.2.

Authentic virus isolation and propagation

Authentic B.1.1.529 was isolated from a specimen from the respiratory tract of a COVID-19 patient in Hong Kong by Kwok-Yung Yuen and colleagues at the Department of Microbiology, The University of Hong Kong. Isolation of wild-type SARS-CoV-2 was previously described[47]. Viruses were propagated in Vero-E6-TMPRSS2 cells and sequence confirmed by next-generation sequencing prior to use.

Authentic virus neutralization assay

To measure neutralization of authentic SARS-CoV-2 viruses, Vero-E6-TMPRSS2 cells were first seeded in 96 well-plates in cell culture media (Dulbecco's Modified Eagle Medium (DMEM) + 10% fetal bovine serum (FBS) + 1% penicillin/streptomycin) overnight at 37 °C under 5% CO_2 to establish a monolayer. The following day, sera or antibodies were serially diluted in 96 well-plates in triplicate in DMEM + 2% FBS and then incubated with 0.01 MOI (multiplicity of infection) of wild-type SARS-CoV-2 or B.1.1.529 at 37 °C for 1 h. Sera were diluted from 1:100 dilution and antibodies were diluted from 10 μg/mL. Afterwards, the mixture was overlaid onto cells and further incubated at 37 °C under 5% CO_2 for approximately 72 h. Cytopathic effects were then scored by plaque assay in a blinded manner. Neutralization curves and IC_{50} values were derived by fitting a non-linear five-parameter dose-response curve to the data in GraphPad Prism version 9.2.

Antibody footprint analysis and RBD mutagenesis analysis

The SARS-CoV-2 spike structure used for displaying epitope footprints and mutations within emerging strains was downloaded from PDB (PDBID: 6ZGE). The structures of antibody-spike complexes were also obtained from PDB (7L5B for 2-15, 6XDG for REGN10933 and REGN10987, 7L2E for 4-18, 7RW2 for 5-7, 7C01 for CB6, 7KMG for LY-COV555, 7CDI for Brii-196, 7KS9 for 910-30, 7LD1 for DH1047, 7RAL for S2X259, 7LSS for 2-7, and 6WPT for S309). Interface residues were identified using PISA[48] using default parameters. The footprint for each antibody was defined by the boundaries of all epitope residues. The border for each footprint was then optimized by ImageMagick 7.0.10-31 (https://imagemagick.org). PyMOL 2.3.2 was used to perform mutagenesis and to make structural plots (Schrödinger).

Reporting summary

Further information on research design is available in the Nature Research Reporting Summary linked to this paper.

Data availability

Materials used in this study will be made available under an appropriate Materials Transfer Agreement. All the data are provided in the paper. The structures used for analysis in this study are available from PDB under IDs 6ZGE, 7L5B, 6XDG, 7L2E, 7RW2, 7C01, 7KMG, 7CDI, 7KS9, 7LD1, 7RAL, 7LSS, and 6WPT.

43. Baym, M. et al. Inexpensive multiplexed library preparation for megabase-sized genomes. *PLoS One* **10**, e0128036, https://doi.org/10.1371/journal.pone.0128036 (2015).
44. Martin, M. Cutadapt Removes Adapter Sequences From High-Throughput Sequencing Reads. *EMBnet.journal* **17**, 10, https://doi.org/10.14806/ej.17.1.200 (2011).
45. Langmead, B. & Salzberg, S. L. Fast gapped-read alignment with Bowtie 2. *Nat Methods* **9**, 357-359, https://doi.org/10.1038/nmeth.1923 (2012).
46. Robinson, J. T. et al. Integrative genomics viewer. *Nat Biotechnol* **29**, 24-26, https://doi.org/10.1038/nbt.1754 (2011).
47. Chu, H. et al. Comparative tropism, replication kinetics, and cell damage profiling of SARS-CoV-2 and SARS-CoV with implications for clinical manifestations, transmissibility, and laboratory studies of COVID-19: an observational study. *Lancet Microbe* **1**, e14-e23, https://doi.org/10.1016/S2666-5247(20)30004-5 (2020).
48. Krissinel, E. & Henrick, K. Inference of macromolecular assemblies from crystalline state. *J Mol Biol* **372**, 774-797, https://doi.org/10.1016/j.jmb.2007.05.022 (2007).

Acknowledgements We are grateful Regeneron Pharmaceuticals, B. Zhang and P. Kwong (NIAID), and B. Dekosky (MIT) for antibodies. This study was supported by funding from the Gates Foundation, JPB Foundation, Andrew and Peggy Cherng, Samuel Yin, Carol Ludwig, David and Roger Wu, Health@InnoHK, and the National Science Foundation (MCB-2032259).

Author contributions D.D.H. conceived this project. L.H.L., S.I., and M.W. conducted pseudovirus neutralization experiments. J.F-W.C., H.C., K.K-H.C., T.T-T.Y., C.Y., K.K-W.T., and H.C. conducted authentic virus neutralization experiments. Y.G. and Z.Z. conducted bioinformatic analyses. L.Y.L. and Y.M.H. constructed the spike expression plasmids. Y.L. managed the project. J.Y. expressed and purified antibodies. M.T.Y. and M.E.S. provided clinical samples. M.S.N. and Y.X.H. contributed to discussions. H.H.W., K-Y.Y., and D.D.H. directed and supervised the project. L.H.L., S.I., and D.D.H. analyzed the results and wrote the manuscript.

Competing interests L.L., S.I., M.S.N., J.Y., Y.H., and D.D.H. are inventors on patent applications (WO2021236998) or provisional patent applications (63/271,627) filed by Columbia University for a number of SARS-CoV-2 neutralizing antibodies described in this manuscript. Both sets of applications are under review. D.D.H. is a co-founder of TaiMed Biologics and RenBio, consultant to WuXi Biologics and Brii Biosciences, and board director for Vicarious Surgical.

Additional information

Supplementary information The online version contains supplementary material available at https://doi.org/10.1038/s41586-021-04388-0.

Correspondence and requests for materials should be addressed to David D. Ho.

Peer review information *Nature* thanks the anonymous reviewers for their contribution to the peer review of this work.

Reprints and permissions information is available at http://www.nature.com/reprints.

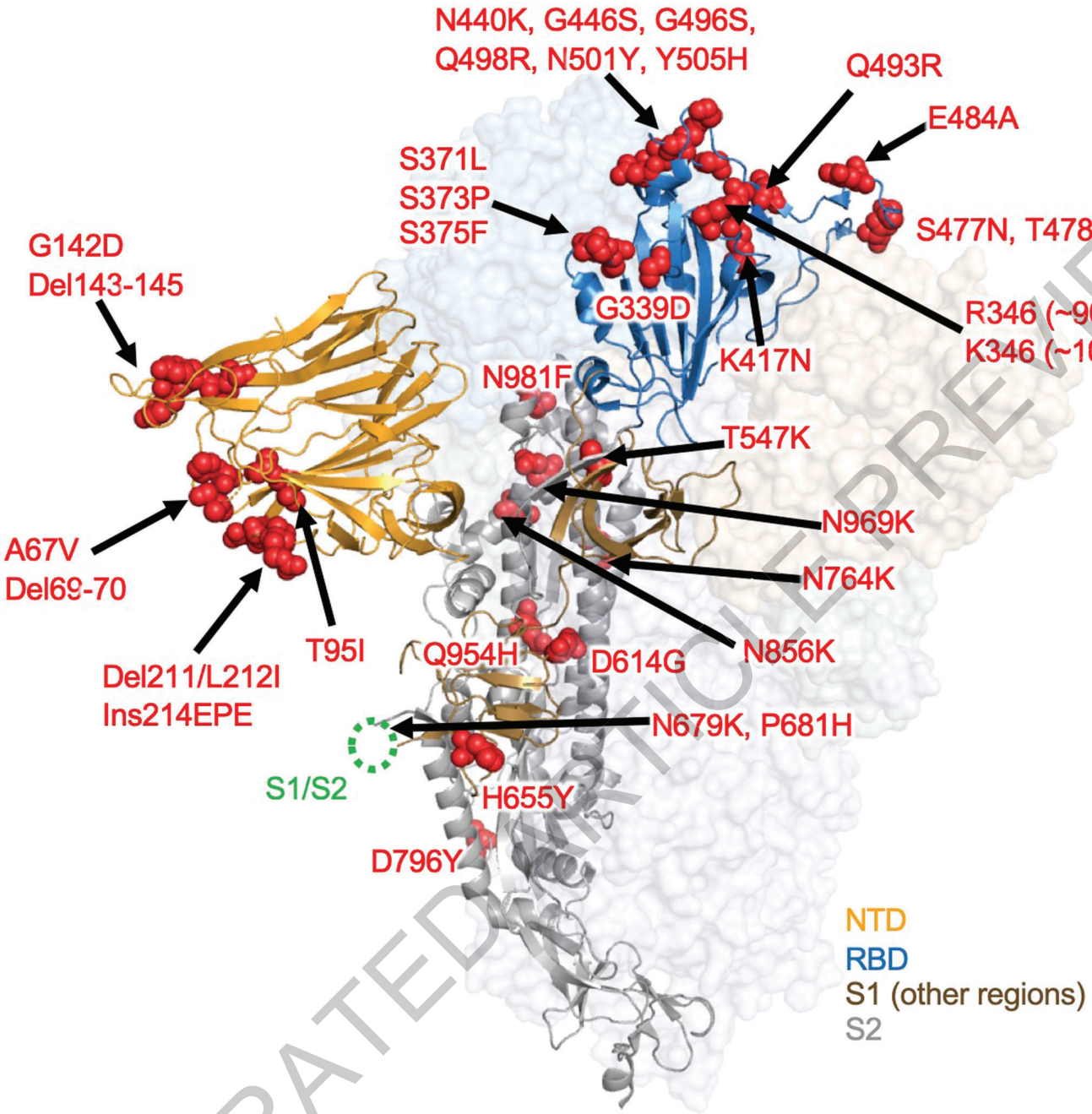

Extended Data Fig. 1 | Mutations within B.1.1.529 denoted on the full SARS-CoV-2 spike trimer. The SARS-CoV-2 spike structure was downloaded from PDB 6ZGE.

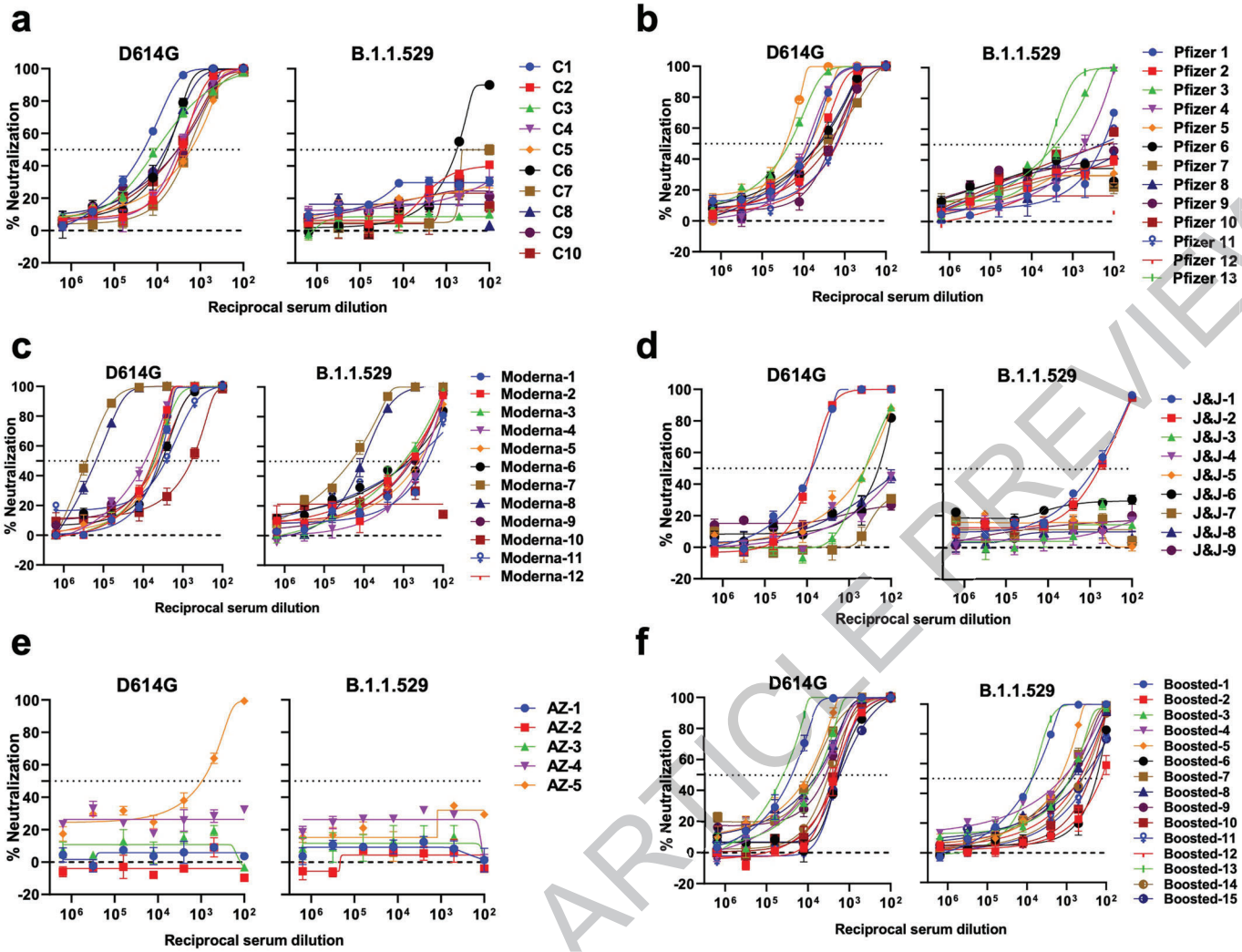

Extended Data Fig. 2 | Individual neutralization curves for pseudovirus neutralization assays by serum. Neutralization by **a**, convalescent sera. **b**, Pfizer (BNT162b2) vaccinee sera. **c**, Moderna (mRNA-1273) vaccinee sera. **d**, J&J (Ad26.COV2.S) vaccinee sera. **e**, AstraZeneca (ChAdOx1 nCoV-19) vaccinee sera. **f**, boosted (three homologous BNT162b2 or mRNA-1273 vaccinations) vaccinee sera. Error bars denote mean ± standard error of the mean (SEM) for three technical replicates.

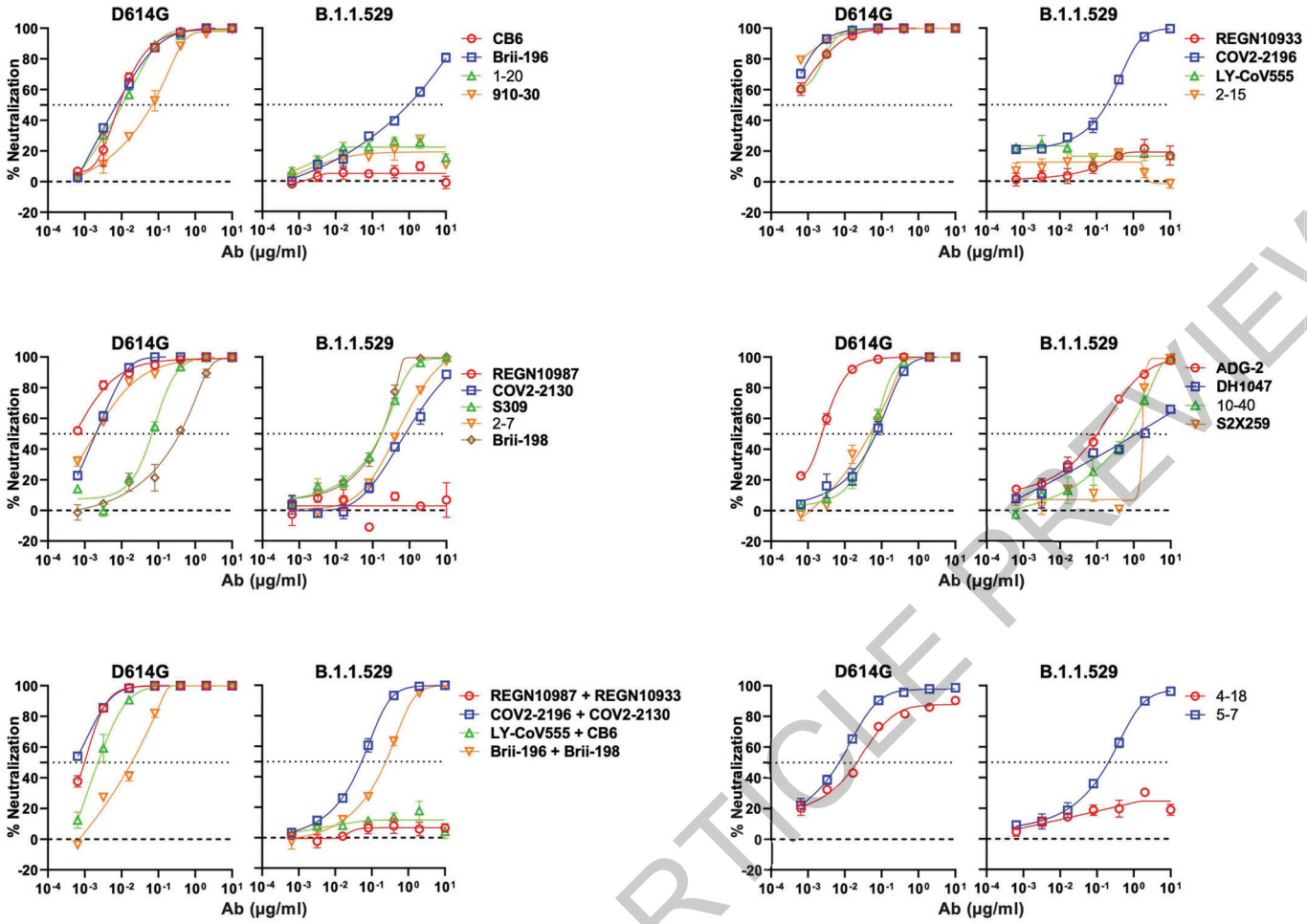

Extended Data Fig. 3 | Individual neutralization curves for pseudovirus neutralization assays by monoclonal antibodies. Error bars denote mean ± standard error of the mean (SEM) for three technical replicates.

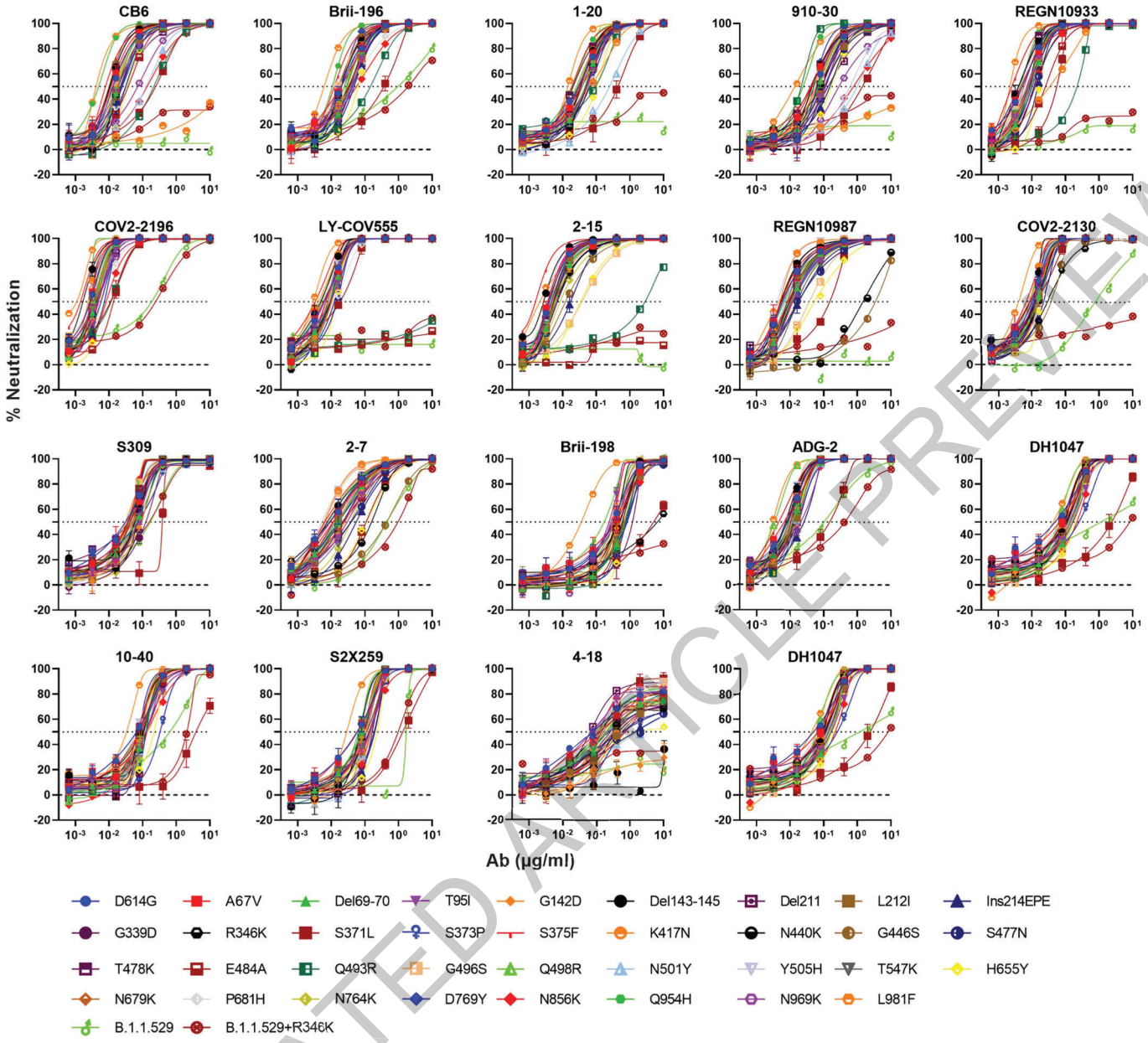

Extended Data Fig. 4 | Individual neutralization curves for pseudovirus neutralization assays by monoclonal antibodies against individual SARS-CoV-2 mutations. Error bars denote mean ± standard error of the mean (SEM) for three technical replicates.

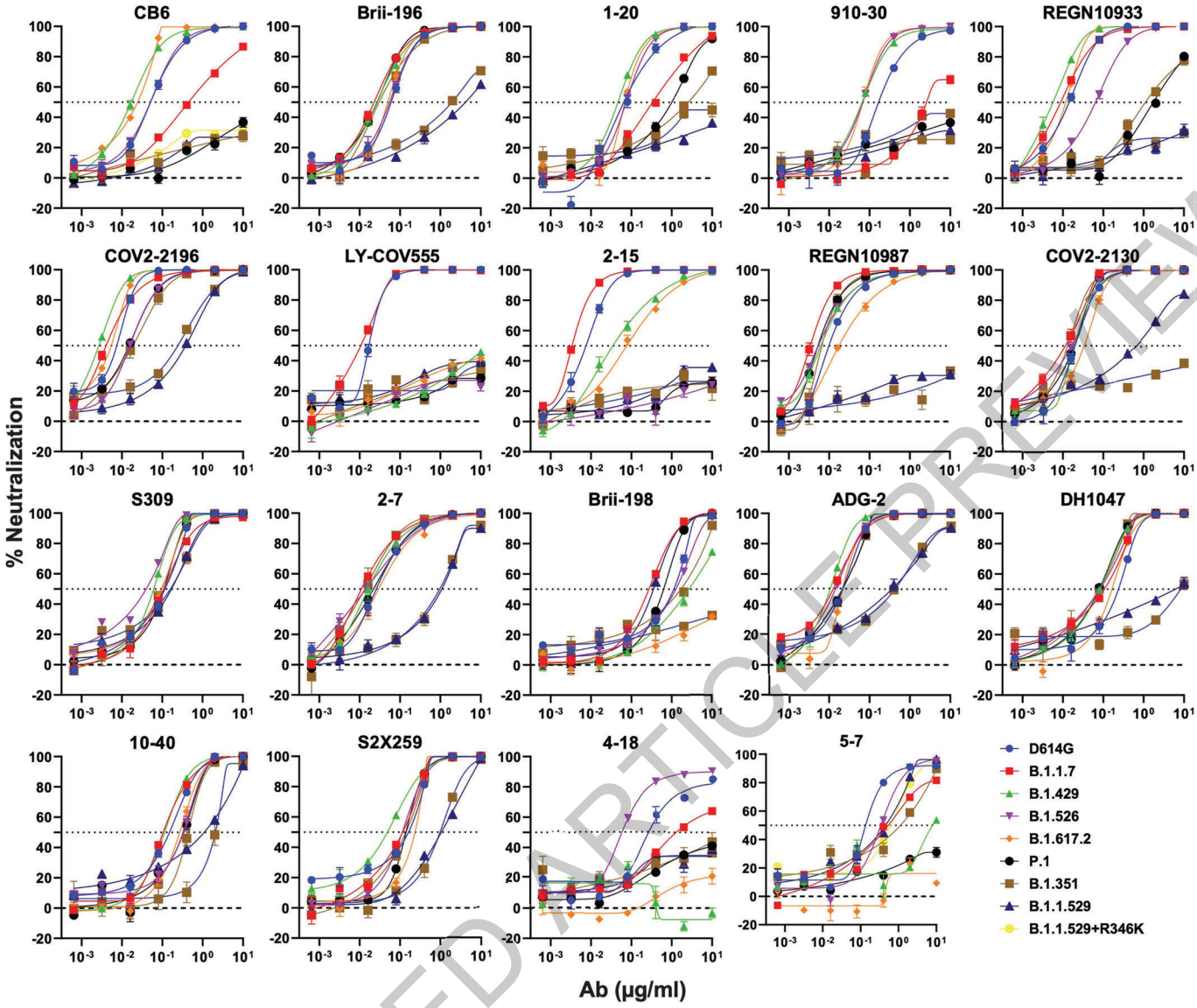

Extended Data Fig. 5 | Individual neutralization curves for pseudovirus neutralization assays by monoclonal antibodies against SARS-CoV-2 variants. Error bars denote mean ± standard error of the mean (SEM) for three technical replicates.

Extended Data Table 1 | Demographics and vaccination information for serum samples from convalescent patients used in this study

Convalescent Sample	Days post-symptoms	Age	Gender
C1	18	57	Female
C2	25	51	Male
C3	29	71	Female
C4	32	50	Male
C5	35	59	Male
C6	120	56	Male
C7	105	54	Female
C8	77	51	Female
C9	18	79	Male
C10	9	45	Male

Extended Data Table 2 | Demographics and vaccination information for serum samples from vaccinated individuals used in this study

Vaccine Sample	Vaccine type	Days post-vaccination (after last dose)	Documented COVID Infection	Age	Gender
Moderna vaccinee #1	mRNA-1273	31	No	72	Male
Moderna vaccinee #2	mRNA-1273	19	No	38	Female
Moderna vaccinee #3	mRNA-1273	6	No	42	Male
Moderna vaccinee #4	mRNA-1273	81	No	40	Female
Moderna vaccinee #5	mRNA-1273	123	No	40	Female
Moderna vaccinee #6	mRNA-1273	177	No	40	Female
Moderna vaccinee #7	mRNA-1273	29	No	57	Female
Moderna vaccinee #8	mRNA-1273	74	No	57	Female
Moderna vaccinee #9	mRNA-1273	32	No	66	Female
Moderna vaccinee #10	mRNA-1273	72	No	63	Male
Moderna vaccinee #11	mRNA-1273	74	No	68	Female
Moderna vaccinee #12	mRNA-1273	58	No	46	Female
Pfizer vaccinee #1	BNT162b2	21	No	62	Male
Pfizer vaccinee #2	BNT162b2	36	No	62	Male
Pfizer vaccinee #3	BNT162b2	26	No	38	Male
Pfizer vaccinee #4	BNT162b2	66	No	38	Male
Pfizer vaccinee #5	BNT162b2	22	No	57	Female
Pfizer vaccinee #6	BNT162b2	61	No	57	Female
Pfizer vaccinee #7	BNT162b2	20	No	55	Male
Pfizer vaccinee #8	BNT162b2	16	No	64	Female
Pfizer vaccinee #9	BNT162b2	32	No	68	Male
Pfizer vaccinee #10	BNT162b2	20	No	35	Male
Pfizer vaccinee #11	BNT162b2	15	No	48	Female
Pfizer vaccinee #12	BNT162b2	21	No	45	Male
Pfizer vaccinee #13	BNT162b2	213	Yes	66	Male
J&J vaccinee #1 (BEI Cat. #NRH-10818)	Ad26.COV2.S	55	Yes	50	Female
J&J vaccinee #2 (BEI Cat. #NRH-10819)	Ad26.COV2.S	61	Yes	50	Female
J&J vaccinee #3 (BEI Cat. #NRH-10835)	Ad26.COV2.S	186	Unknown	43	Female
J&J vaccinee #4 (BEI Cat. #NRH-10845)	Ad26.COV2.S	69	Unknown	28	Female
J&J vaccinee #5 (BEI Cat. #NRH-10823)	Ad26.COV2.S	50	No	42	Female
J&J vaccinee #6 (BEI Cat. #NRH-10834)	Ad26.COV2.S	175	Unknown	43	Female
J&J vaccinee #7 (BEI Cat. #NRH-10839)	Ad26.COV2.S	39	No	47	Male
J&J vaccinee #8 (BEI Cat. #NRH-10844)	Ad26.COV2.S	60	Unknown	28	Female
J&J vaccinee #9 (BEI Cat. #NRH-10824)	Ad26.COV2.S	51	No	43	Male
AZ vaccinee #1 (BEI Cat. #NRH-10817)	ChAdOx1 nCoV-19	158	Unknown	73	Male
AZ vaccinee #2 (BEI Cat. #NRH-10814)	ChAdOx1 nCoV-19	152	Unknown	36	Female
AZ vaccinee #3 (BEI Cat. #NRH-10815)	ChAdOx1 nCoV-19	159	Unknown	36	Female
AZ vaccinee #4 (BEI Cat. #NRH-10811)	ChAdOx1 nCoV-19	142	Yes	26	Female
AZ vaccinee #5 (BEI Cat. #NRH-3083)	ChAdOx1 nCoV-19	91	Unknown	56	Female
Boosted sera #1	mRNA-1273/mRNA-1273	28	No	66	Female
Boosted sera #2	BNT162b2/BNT162b2	30	No	68	Male
Boosted sera #3	BNT162b2/BNT162b2	14	No	64	Female
Boosted sera #4	BNT162b2/BNT162b2	34	No	55	Male
Boosted sera #5	BNT162b2/BNT162b2	34	No	45	Male
Boosted sera #6	BNT162b2/BNT162b2	15	No	50	Female
Boosted sera #7	BNT162b2/BNT162b2	15	No	48	Female
Boosted sera #8	BNT162b2/BNT162b2	29	No	71	Male
Boosted sera #9	BNT162b2/BNT162b2	90	No	59	Male
Boosted sera #10	BNT162b2/BNT162b2	33	No	45	Male
Boosted sera #11	BNT162b2/BNT162b2	87	No	66	Female
Boosted sera #12	BNT162b2/BNT162b2	84	No	26	Male
Boosted sera #13	mRNA-1273/mRNA-1273	23	No	28	Female
Boosted sera #14	BNT162b2/BNT162b2	14	No	78	Male
Boosted sera #15	BNT162b2/BNT162b2	14	No	75	Female

Extended Data Table 3 | Oligos used to construct spike expression plasmids

Oligo name	Targeted mutations	Oligo sequence
O_single_mutant1	A67V	ATGTGACCTGGTTCCATGTGATCCATGTGTCTGGCACCAATGGCACC
O_single_mutant2	Del69-70	CTGGTTCCATGCCATCTCTGGCACCAATGGCAC
O_single_mutant3	T95I	CTTTGCCAGCATCGAGAAGAGCAACATCATC
O_single_mutant4	Del143-145	TGTAATGACCCATTCCTGGGACACAAGAACAACAAGTCCTGGATG
O_single_mutant5	G142D	GTAATGACCCATTCCTGGACGTCTACTACCACAAG
O_single_mutant6	Del211	ACACACACCAATCCTGGTGAGGGACCTG
O_single_mutant7	L212I	CACACCAATCAACATCGTGAGGGACCTGCC
O_single_mutant8	Ins214EPE	ACCAATCAACCTGGTGAGGGAGCCCGAGGACCTGCCACAGGGCTT
O_single_mutant9	G339D	CTGTGTCCATTTGACGAGGTGTTCAATGCCAC
O_single_mutant10	R346K	TGTTCAATGCCACCAAGTTTGCCTCTGTCTATGCCTG
O_single_mutant11	S371F	CTCTGTGCTCTACAACTTTGCCTCCTTCAGCAC
O_single_mutant12	S371L	CTCTGTGCTCTACAACCTGGCCTCCTTCAGCAC
O_single_mutant13	S373P	CTCTACAACTCTGCCCCCTTCAGCACCTTCAAG
O_single_mutant14	S375F	CAACTCTGCCTCCTTCTTCACCTTCAAGTGTTATGG
O_single_mutant15	K417N	CCCCTGGACAAACAGGCAACATTGCTGACTACAACTACAAACTGC
O_single_mutant16	N440K	CCTGGAACAGCAACAAGCTGGACAGCAAGGTG
O_single_mutant17	G446S	GGACAGCAAGGTGAGCGGCAACTACAACTAC
O_single_mutant18	S477N	GATTTACCAGGCTGGCAACACACCATGTAATG
O_single_mutant19	T478K	CAGGCTGGCAGCAAGCCATGTAATGGAGTGGA
O_single_mutant20	E484A	GTAATGGAGTGGCCGGCTTCAACTGTTAC
O_single_mutant21	Q493R	GTTACTTTCCACTCAGATCCTATGGCTTCCAAC
O_single_mutant22	G496S	CACTCCAATCCTATAGCTTCCAACCAACCAATG
O_single_mutant23	Q498R	CAATCCTATGGCTTCAGACCAACCAATGGAGTGGG
O_single_mutant24	N501Y	CTTCCAACCAACCTACGGAGTGGGCTACCAACC
O_single_mutant25	Y505H	AATGGAGTGGGCCACCAACCATACAGG
O_single_mutant26	T547K	CTTCAATGGACTGAAGGGCACAGGAGTGCTGAC
O_single_mutant27	H655Y	CTGATTGGAGCAGAGTACGTGAACAACTCCTATG
O_single_mutant28	N679K	CCAGACCCAGACCAAGAGCCCAAGGAGGGCA
O_single_mutant29	P681H	CCCAGACCAACAGCAGAAGGAGGGCAAGGTCTGTGGC
O_single_mutant30	N764K	GTACCCAACTTAAGAGGGCTCTGACAGGC
O_single_mutant31	D769Y	GACACCTCCAATCAAGTACTTTGGAGGCTTC
O_single_mutant32	N856K	GTGCCCAGAAGTTCAAGGGACTGACAGTGCTG
O_single_mutant33	Q954H	CAAGATGTGGTGAACCACAATGCCCAGGCTCTG
O_single_mutant34	N969K	GCAACTTTCCAGCAAGTTTGGAGCCATCTCCTC
O_single_mutant35	L981F	GTGCTGAATGACATCTTCAGCAGACTGGACAAGGTGGAGG
O_multiple_oligo1	A67V, Del69-70	TGGTTCCATGTGATCTCTGGCACCAATGG
O_multiple_oligo2	T95I	CTTTGCCAGCATCGAGAAGAGCAAC
O_multiple_oligo3	G142D, Del143-145	GACCCATTCCTGGACCACAAGAACAACAAGTC
O_multiple_oligo4	L212I, Ins214EPE	CACACACCAATCATCGTGAGGGAGCCCGAGGACCTGCCACAGGGCTTC
O_multiple_oligo5	G339D	TGTGTCCATTTGACGAGGTGTTCAATG
O_multiple_oligo6	S371L, S373P, S375F	TGTGCTCTACAACCTGGCCCCCTTCTTCACCTTCAAGTGTTATG
O_multiple_oligo7	K417N	GGACAAACAGGCAACATTGCTGACTACA
O_multiple_oligo8	N440K, G446S	GCAACAAGCTGGACAGCAAGGTGAGCGGCAACTACAA
O_multiple_oligo9	S477N, T478K, E484A	ACCAGGCTGGCAACAAGCCATGTAATGGAGTGGCCGGCTTCAACTGT
O_multiple_oligo10	Q493R, G496S, Q498R, N501Y, Y505H	TACTTTCCACTCAGATCCTATAGCTTCAGACCAACCTACGGAGTGGGCCACCAACCATACAGG GTGGTGGTGCTGTCCTTTGA
O_multiple_oligo11	T547K	GGACTGAAGGGCACAGGAG
O_multiple_oligo12	D614G	CTCTACCAGGGCGTGAACTGTAC
O_multiple_oligo13	H655Y	TTGGAGCAGAGTACGTGAACAACTC
O_multiple_oligo14	N679K, P681H	CAGACCAAGAGCCACAGGAGGGCAAGG
O_multiple_oligo15	N764K	CCAACTTAAGAGGGCTCTGACAG
O_multiple_oligo16	D796Y	CCTCCAATCAAGTACTTTGGAGGCTTC
O_multiple_oligo17	N856K	CAGAAGTTCAAGGGACTGACAGTGCTG
O_multiple_oligo18	Q954H	GTGGTGAACCACAATGCCCAGGCTC
O_multiple_oligo19	N969K	AACTTTCCAGCAAGTTTGGAGCCATCTCCTC
O_multiple_oligo20	L981F	AATGACATCTTCAGCAGACTGGACAAGGTGGAGGCTGAGGTCCAGATTG

nature portfolio

Corresponding author(s): David D. Ho

Last updated by author(s): Dec 20, 2021

Reporting Summary

Nature Portfolio wishes to improve the reproducibility of the work that we publish. This form provides structure for consistency and transparency in reporting. For further information on Nature Portfolio policies, see our Editorial Policies and the Editorial Policy Checklist.

Statistics

For all statistical analyses, confirm that the following items are present in the figure legend, table legend, main text, or Methods section.

n/a	Confirmed
☐	☒ The exact sample size (*n*) for each experimental group/condition, given as a discrete number and unit of measurement
☐	☒ A statement on whether measurements were taken from distinct samples or whether the same sample was measured repeatedly
☐	☒ The statistical test(s) used AND whether they are one- or two-sided *Only common tests should be described solely by name; describe more complex techniques in the Methods section.*
☒	☐ A description of all covariates tested
☒	☐ A description of any assumptions or corrections, such as tests of normality and adjustment for multiple comparisons
☐	☒ A full description of the statistical parameters including central tendency (e.g. means) or other basic estimates (e.g. regression coefficient) AND variation (e.g. standard deviation) or associated estimates of uncertainty (e.g. confidence intervals)
☐	☒ For null hypothesis testing, the test statistic (e.g. *F*, *t*, *r*) with confidence intervals, effect sizes, degrees of freedom and *P* value noted *Give P values as exact values whenever suitable.*
☒	☐ For Bayesian analysis, information on the choice of priors and Markov chain Monte Carlo settings
☒	☐ For hierarchical and complex designs, identification of the appropriate level for tests and full reporting of outcomes
☒	☐ Estimates of effect sizes (e.g. Cohen's *d*, Pearson's *r*), indicating how they were calculated

Our web collection on statistics for biologists contains articles on many of the points above.

Software and code

Policy information about availability of computer code

Data collection	SoftMax Pro 7.0.2 (Molecular Devices, LLC) was used to measure luminescence in the pseudovirus neutralization assays.
Data analysis	GraphPad Prism (version 9.2) was used for data visualization and for statistical tests. Cutadapt (version 2.1) was used for processing of raw reads from next-generation sequencing. Bowtie2 (version 2.3.4) was used for alignment of reads to sequences. PISA was used for identifying antibody-spike interface residues. Antibody footprints were optimized by ImageMagick 7.0.10-31. PyMOL (version 2.3.2) was used for RBD mutagenesis analysis and for visualization.

For manuscripts utilizing custom algorithms or software that are central to the research but not yet described in published literature, software must be made available to editors and reviewers. We strongly encourage code deposition in a community repository (e.g. GitHub). See the Nature Portfolio guidelines for submitting code & software for further information.

Data

Policy information about availability of data

All manuscripts must include a data availability statement. This statement should provide the following information, where applicable:

- Accession codes, unique identifiers, or web links for publicly available datasets
- A description of any restrictions on data availability
- For clinical datasets or third party data, please ensure that the statement adheres to our policy

Materials used in this study will be made available under an appropriate Materials Transfer Agreement. All the data are provided in the paper. The structures used for analysis in this study are available from PDB under IDs 6ZGE, 7L5B, 6XDG, 7L2E, 7RW2, 7C01, 7KMG, 7CDI, 7KS9, 7LD1, 7RAL, 7LSS, and 6WPT.

Field-specific reporting

Please select the one below that is the best fit for your research. If you are not sure, read the appropriate sections before making your selection.

☒ Life sciences ☐ Behavioural & social sciences ☐ Ecological, evolutionary & environmental sciences

For a reference copy of the document with all sections, see nature.com/documents/nr-reporting-summary-flat.pdf

Life sciences study design

All studies must disclose on these points even when the disclosure is negative.

Sample size	We used similar sample sizes as in previous work (e.g. Wang et al 2021, Nature), which we had previously determined to be sufficient sample sizes for comparisons between groups for these experiments.
Data exclusions	No data were excluded.
Replication	The key results, the resistance of R346K, S371L, B.1.1.529, and B.1.1.529+R346K to monoclonal antibodies in pseudoviruses, and serum neutralization of authentic viruses, were repeated twice independently in technical triplicate with similar results. The results that are shown are representative. Other experiments were conducted in technical triplicate and not repeated.
Randomization	As this is an observational study, randomization is not relevant.
Blinding	As this is an observational study, investigators were not blinded.

Reporting for specific materials, systems and methods

We require information from authors about some types of materials, experimental systems and methods used in many studies. Here, indicate whether each material, system or method listed is relevant to your study. If you are not sure if a list item applies to your research, read the appropriate section before selecting a response.

Materials & experimental systems

n/a	Involved in the study
☐	☒ Antibodies
☐	☒ Eukaryotic cell lines
☒	☐ Palaeontology and archaeology
☒	☐ Animals and other organisms
☐	☒ Human research participants
☒	☐ Clinical data
☒	☐ Dual use research of concern

Methods

n/a	Involved in the study
☒	☐ ChIP-seq
☒	☐ Flow cytometry
☒	☐ MRI-based neuroimaging

Antibodies

Antibodies used	All of the antibodies used in this study were produced in our laboratory or received from other laboratories. 1-20, 2-15, S309, 2-7, ADG-2, DH1047, 10-40, S2X259, 4-18, and 5-7 were expressed and purified in-house as described previously in Liu et al 2020, Nature. REGN10987, REGN10933, COV2-2196, and COV2-2130 were provided by Regeneron Pharmaceuticals, Brii-196 and Brii-198 were provided by Brii Biosciences, CB6 was provided by Baoshan Zhang and Peter Kwong (NIH), and 910-30 was provided by Brandon DeKosky (MIT).
Validation	All of the antibodies have been validated in previous studies both by binding to SARS-CoV-2 spike and neutralization of SARS-CoV-2 (both pseudovirus and authentic virus), and when applicable, have been confirmed to give similar results as that described in publications by other groups. Specifically, 1-20 and 4-18 were tested in Liu et al 2020, Nature, CB6, Brii-196, 910-30, REGN10933, COV2-2196, LY-CoV555, 2-15, REGN10987, COV2-2130, S309, 2-7, Brii-198, and 5-7 were tested in Wang et al 2021, Nature, and ADG-2, DH1047, 10-40, and S2X259 were tested in Liu et al 2021, bioRxiv.

Eukaryotic cell lines

Policy information about cell lines

Cell line source(s)	Expi293 cells were obtained from Thermo Fisher (Catalog #A14527), Vero E6 cells were obtained from ATCC (Catalog# CRL-1586), HEK293T cells were obtained from ATCC (Catalog# CRL-3216), and Vero-E6-TMPRSS2 cells were obtained from JCRB (Catalog# JCRB1819).
Authentication	Cell lines were purchased from authenticated vendors, and morphology was also confirmed visually prior to use.

Mycoplasma contamination	Cell lines tested mycoplasma negative.
Commonly misidentified lines (See ICLAC register)	No commonly misidentified cell lines were used in this study.

Human research participants

Policy information about studies involving human research participants

Population characteristics	Population characteristics are described in detail for each individual in Extended Data Table 1 and 2. Convalescent samples had the following ranges: 9-120 days post-symptoms, 45-79 years old, 4/10 female, 6/10 male. We presume all of these individuals were infected with the wild-type strain of SARS-CoV-2 as these samples were collected in Spring of 2020. Vaccinee samples had the following ranges: 6-213 days post-vaccination, 26-78 years old, 12/54 two mRNA-1273 vaccinations, 13/54 two BNT162b2 vaccinations, 9/54 Ad26.COV2.S vaccination, 5/54 two ChAdOx1 nCoV-19 vaccinations, 2/54 three mRNA-1273 vaccinations, 13/54 three BNT162b2 vaccinations, 4/54 previously infected, 8/54 unknown previous infection status, 42/54 uninfected, 31/54 female, 23/54 male.
Recruitment	For convalescent sera, convalescing patients volunteered and were enrolled in an observational cohort study at Columbia University Irving Medical Center in Spring of 2020. For the BNT162b2 and mRNA-1273 vaccinee sera, individuals volunteered and were enrolled in an observational cohort study at Columbia University Irving Medical Center to study the immunological responses to SARS-CoV-2 in individuals who had received COVID-19 vaccines. Ad26.COV2.S and ChAdOx1 nCoV-19 vaccinee serum samples were received from BEI Resources. Self-selection biases may have affected the demographics of the enrolled population, but are not expected to have impacted the results of this study. High titer samples were specifically chosen within each of the serum groups so that fold-change in titer could be better determined, as also discussed in the manuscript.
Ethics oversight	All collections were conducted under protocols reviewed and approved by the Institutional Review Board of Columbia University. All participants provided written informed consent.

Note that full information on the approval of the study protocol must also be provided in the manuscript.